Microvascular Research 80 (2010) 394–401

Contents lists available at ScienceDirect

Microvascular Research

journal homepage: www.elsevier.com/locate/ymvre

Regular Article

Composition of the endothelial glycocalyx and its relation to its thickness and diffusion of small solutes

Lujia Gao, Herbert H. Lipowsky *

Department of Bioengineering, The Pennsylvania State University, University Park, PA 16802, USA

ARTICLE INFO

Article history:
Received 26 April 2010
Revised 13 June 2010
Accepted 14 June 2010
Available online 21 June 2010

Keywords:
Glycocalyx
Glycosaminoglycans
Glycocalyx thickness
Diffusion coefficient
Lectin binding
fMLP
Inflammation

ABSTRACT

The endothelial glycocalyx is well endowed with the glycosaminoglycans (GAGs) heparan sulfate, chondroitin sulfate and hyaluronan. The current studies aimed to assess the relative contributions of each of these GAGs to the thickness and permeability of the glycocalyx layer by direct enzymatic removal of each using micropipettes to infuse heparinase, chondroitinase and hyaluronidase into post-capillary venules of the intestinal mesentery of the rat. The relative losses of GAGs due to enzymatic removal were compared with stimulated shedding of glycans induced by superfusing the mesentery with 10^{-7} M fMLP. Thickness of the glycocalyx was assessed by infiltration of the glycocalyx with circulating FITC labeled 70 kDa dextran (Dx70) and measuring the distance from the dye front to the surface of the endothelium (EC), which averaged 463 nm under control conditions. Reductions in thickness were 43.3%, 34.1% and 26.1% following heparinase, chondroitinase and hyaluronidase, respectively, and 89.7% with a mixture of all three enzymes. Diffusion coefficients of FITC in the glycocalyx were determined using a 1-D diffusion model. By comparison of measured transients in radial intensity of a bolus of FITC with that of a computational model a diffusion coefficient D was obtained. Values of D were obtained corresponding to the thickness of the layer demarcated by Dx70 (D_{Dx70}), and a smaller sublayer 173 nm above the EC surface (D_{173}), prior to and following enzyme infusion and superfusion with fMLP. The magnitude of D_{Dx70} was twice that of D_{173} suggesting that the glycocalyx is more compact near the EC surface. Chondroitinase and hyaluronidase significantly increased both D_{Dx70} and D_{173}. However, heparinase decreased D_{Dx70}, and did not induce any significant change for the D_{173}. These observations suggest that the three GAGs are not evenly distributed throughout the glycocalyx and that they each contribute to permeability of the glycocalyx to a differing extent. The fMLP-induced shedding caused a reduction in glycocalyx thickness (which may increase permeability) and as with heparinase, decreased the diffusion coefficient of solutes (which may decrease permeability). This behavior suggests that the removal of heparan sulfate may cause a collapse of the glycocalyx which counters decreases in thickness by compacting the layer to maintain a constant resistance to filtration.

Introduction

The luminal surface of endothelial cells is endowed with a carbohydrate-rich surface layer referred to as the endothelial glycocalyx. It has been shown to be an important barrier to transvascular exchange of water and solutes (Adamson, 1990; Henry and Duling, 1999) and sieving of plasma-borne macromolecules (Huxley and Williams, 2000; van Haaren et al., 2003; Vink and Duling, 2000). The glycocalyx has been shown to be a physiologically significant binding site for antithrombin III, tissue factor pathway inhibitors, lipoprotein lipase, vascular endothelial growth factor, fibroblast growth factor, and extracellular superoxide dismutase (Reitsma et al., 2007). The glycocalyx has also been shown to serve as a barrier to leukocyte–endothelium adhesion (Mulivor and Lipowsky, 2002), shear stress sensor and regulator of mechanotransduction (Florian et al., 2003).

Studies have explored the fine structure of the glycocalyx and its potential impact on permeability using techniques of electron microscopy (Squire et al., 2001; Van den Berg et al., 2003), intravital microscopy (Henry and Duling, 1999; Vink and Duling, 2000) and mathematical modeling (Stace and Damiano, 2001; Sugihara-Seki et al., 2008; Weinbaum et al., 2003). It has been suggested that the glycocalyx is a porous layer composed of a matrix of molecules that are arranged in a regular pattern (Squire et al., 2001). The most prominent components of the glycocalyx are the glycosaminoglycans (GAGs) heparan sulfate (HS), chondroitin sulfate (CS) and hyaluronan (HA). Both HS and CS carry negatively charged sulfate groups and are covalently linked to transmembrane proteoglycans (PGs). The GAG-carrying ability of PGs and glycoproteins can be variable (Reitsma et al., 2007) and carry multiple chains of HS and CS. The ratio of HS to

* Corresponding author. Department of Bioengineering, Penn State University, 205 Hallowell Building, University Park, PA 16802, USA. Fax: +1 814 863 0490.
E-mail address: hhlbio@engr.psu.edu (H.H. Lipowsky).

0026-2862/$ – see front matter © 2010 Elsevier Inc. All rights reserved.
doi:10.1016/j.mvr.2010.06.005

CS chains has been shown to be on the order of 4:1, respectively (Rapraeger, 1989) and their sulfation level may change depending on the physiological micro-environment (Rapraeger, 1989; Vogl-Willis and Edwards, 2004). HA is the only GAG that has no sulfate groups and is not covalently linked to any proteins (Laurent and Fraser, 1992).

Both HS and CS are synthesized inside the Golgi apparatus, whereas HA synthases (HASs) are plasma membrane associated such that newly synthesized HA strands are extruded outside the cell (Prehm, 1989). There are several ways for HA to be integrated into the glycocalyx. The primary HA receptor in the glycocalyx is thought to be CD44 (Aruffo et al., 1990) along with HA binding protein (Toole, 1990). HA chains can be self-assembled by steric interaction into random fibrous networks (Scott and Heatley, 1999). Besides GAG-carrying proteoglycans, blood-borne soluble proteins are also important components of the glycocalyx, shown experimentally to be decreased by removing plasma proteins (Adamson and Clough, 1992; Huxley and Curry, 1991). Under normal physiological conditions, the structure of the glycocalyx layer is fairly stable but its molecular contents represent a dynamic balance between biosynthesis of new glycans and shear dependent removal of existing constituents (Mulivor and Lipowsky, 2004).

The endothelial glycocalyx has been shown to be shed in response to inflammation (Henry and Duling, 2000; Mulivor and Lipowsky, 2004), hyperglycemia (Zuurbier et al., 2005), endotoxemia and septic shock (Hofmann-Kiefer et al., 2009), presence of oxidized LDL (Constantinescu et al., 2001), TNFα (Chappell et al., 2009), atrial natriuretic peptide (Bruegger et al., 2005), abnormal blood shear stress (Gouverneur et al., 2006; Haldenby et al., 1994), ischemia-reperfusion injury (Mulivor and Lipowsky, 2004), and during by-pass surgery (Rehm et al., 2007; Svennevig et al., 2008). These observations have lead to the hypothesis of an underlying connection between integrity of the glycocalyx and vascular homeostasis (Mulivor and Lipowsky, 2004; Zuurbier et al., 2005). The exact cellular signaling cascades between these pathological conditions and shedding of the glycocalyx are not yet fully understood. However, evidence suggests that several key enzymes, such as the matrix metalloproteases, are directly responsible for shedding of the glycocalyx components (Mulivor and Lipowsky, 2009).

The present studies were undertaken to explore the relative contribution of each of these three principal GAGs to the apparent thickness of the glycocalyx and its permeability to small solutes in post-capillary venules of the rat intestinal mesentery. Thickness of the glycocalyx (δ) was assessed using established techniques of macromolecule exclusion (Vink and Duling, 1996) and permeability to small solutes (namely the fluorescent dye FITC) was determined by direct measurement of its diffusion through the EC surface layer and fitting the observed variations to a mathematical model based upon an apparent diffusion coefficient, D. Changes in δ and D were determined following enzymatic removal of selected GAGs by direct infusion of heparinase, chondroitinase and hyaluronidase in post-capillary venules using micropipettes.

Materials and methods

Animal preparation and intravital microscopy

Adequate measures were taken to minimize pain or discomfort, and all experiments were conducted in accordance with international standards on animal welfare and compliant with local and national regulations. Male Wistar rats, weighing 200–300 g, were anesthetized using Inactin (135 mg/kg, i.p.). A tracheostomy was performed to facilitate spontaneous respiration. The right internal jugular vein was cannulated with PE50 tubing for systemic administration of anesthetic. Arterial blood pressure was monitored by means of a cannula in the left carotid artery connected to a strain-gage pressure transducer and monitored to assess depth of anesthesia. Rectal temperature was monitored to control a heating pad using a closed-loop automatic controller set to maintain core body temperature at 37° C. The terminal ileum was exteriorized through a mid-line abdominal incision and draped over a clear glass pedestal for viewing the mesentery by intravital microscopy. Surrounding tissues were covered with sterile cotton gauze and irrigated with warmed (37° C) Hepes-buffered (pH = 7.4) Ringer's solution. Post-capillary venules were selected for microscopic observation under bright field or fluorescent epi-illumination, using a Zeiss 40x/0.75NA water immersion objective. Video recordings of post-capillary venules were digitized with a PCO 1600 digital CCD camera (PCO Imaging, Germany) at a spatial resolution of 1600 × 1200 pixels with a depth of 14 bits for subsequent analysis. The effective magnification yielded a pixel spacing of 17.3 pixels/μm. Calibration studies under fluorescence illumination revealed that pixel intensity was linearly related to fluorophore concentration within a 5% RMS error.

Cannulation of post-capillary venules

Glass micropipettes (1 mm OD, WPI, Sarasota, FL) were pulled using a pipette puller (Model 700C, David Kopf Instruments, Tujunga, CA) and double-beveled to obtain a sharply angled 2–5 μm tip opening using a pipette beveler (BV-10, Sutter Instrument Co., Novato, CA). The tip region of each micropipette was filled by capillarity with heparinized (5 U/mL) normal saline and the remainder of the lumen back filled with specific solutions, depending upon the protocol. The micropipette was held in a pipette holder which was connected to a syringe using silicon tubing. The pipette holder and silicon tubing were filled with water and the back end connected to a pressurized reservoir to enable infusion. The pipette holder was mounted on a hydraulic micro-manipulator (MMH-1, Narishige, Japan). Depending on specific protocols, a proximal feeding branch of the venule under observation was cannulated for infusion, as depicted in the schematic of the experimental protocol shown in Fig. 1. The syringe was pressurized to obtain a flow rate comparable to the pre-intubation undisturbed flow by increasing the infusion pressure such that the dividing streamline in the confluent streams was maintained at its pre-intubation position.

Preparation of fluorophores and enzymes

Post-capillary venules were perfused with three fluorescent molecules: (1) The lectin BS1, labeled with Alexa Fluor-488, to study glycan shedding and enzymatic removal, (2) Fluorescein

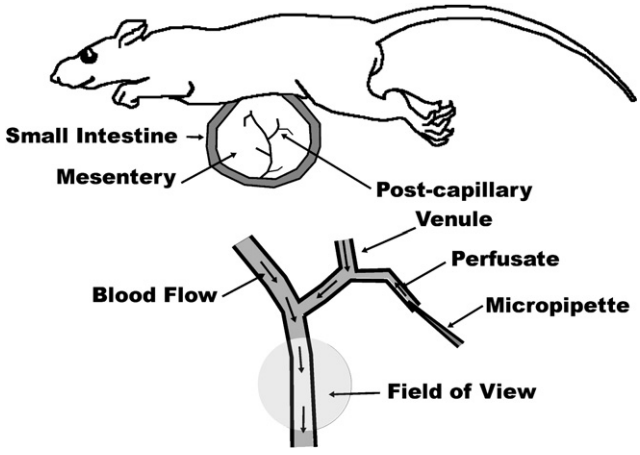

Fig. 1. Schematic of the experiment protocol. A post-capillary venule in the exteriorized rat mesentery was selected for intravital microscopic observation. An upstream branch was cannulated with a micropipette for perfusion with Alexa labeled BS-1 lectin to label the glycocalyx, or enzymes for GAG degradation. Fluorescence intensity of the endothelial surface was acquired to quantify glycan shedding.

isothiocyanate (FITC) labeled 70 kDa dextran (Dx70), to obtain a measure of the thickness of the glycocalyx, and free FITC, for determination of its diffusion coefficient within the glycocalyx. The lectin BS1 (L2380, Sigma, St. Louis, MO) was conjugated with Alexa Fluor 488 (A20000, Invitrogen, Eugene, OR) to yield 2.7 mole of fluorophore per mole BS1, and its concentration adjusted to 1% in PBS. FITC–Dextran 70 kDa (FD-70S, Sigma) was dissolved in PBS to make a 0.1% solution. Prior to each experiment, FITC–Dx70 solution was centrifuged at 16000*g* for 5 min to remove particulates and then filtered through a 0.26 μm polycarbonate syringe filter. FITC (F7250, Sigma) was solubilized (1%) in PBS and the pH adjusted to 7.4 for direct infusion in post-capillary venules.

Enzymes used to cleave specific GAGs included heparinase III (50 U/mL in PBS, H8891, Sigma), chondroitinase ABC (10 U/mL in PBS, C2905, Sigma) and hyaluronidase (3000 U/mL in PBS, H3631, Sigma). All enzyme solutions were applied to selected post-capillary venules for a 10 min perfusion via micropipette. To ensure maximal digestion, in separate studies concentration and perfusion duration were doubled to demonstrate that no significant additional effects occurred for all three enzymes (data not shown).

Measurement of BS1-GAG binding

To examine enzymatic removal of components of the glycocalyx, BS1 was used, which has been shown to bind to all three principal GAGs, HS, CS and HA (Schnitzer et al., 1990). BS1-Alexa solution was infused via micropipettes for 10 min, following which the micropipette was withdrawn and normal blood flow allowed to resume. Following washout of non-bound fluorophore, the venule was re-intubated with a micropipette for perfusion with enzyme solutions for 10 min to cleave specific GAGs. Video recordings of BS1 bound to the EC surface were taken 20–30 min following BS1 infusion, following which recordings were taken again prior to 10 min infusion of enzymes. A third set of video recordings was taken 10 min following completion of the enzyme infusion, which occurred on average 30–40 min after the end of the BS1 perfusion. Control measurements in the absence of enzyme treatment were taken 40 min following BS1 perfusion to obtain a non-stimulated reference for subsequent measurements.

The method for quantifying the extent of BS1-Alexa binding to the EC is illustrated in Fig. 2 for a representative post-capillary venule in both brightfield (Fig. 2A) and fluorescence (Fig. 2B) illumination. In this particular venule, the infused BS1-Alexa solution stream was confined to the left venular wall (Fig. 2B). The luminal surface of the EC was identified as the outer edge of the dark refractive band in the brightfield image. BS1 staining appears on the luminal side of the EC. A measurement line was drawn along the center of the fluorescent band and the average fluorescence intensity was recorded in a region of interest along this line bounded by the edges of the band, which typically spanned about 500 nm on either side of the line.

Measurement of glycocalyx thickness using FITC–Dx70

The thickness of the glycocalyx layer was estimated by measuring the distance between the luminal surface of the EC and the edge of circulating FITC–Dx70, introduced into the systemic circulation (0.1% in 0.15 mL) via the jugular vein cannula. After completion of the bolus infusion, brightfield images were taken of selected post-capillary venules, in a focal plane where the dark refractive band at the EC luminal surface was sharply in focus. The microscope was then switched to fluorescence epi-illumination and video scenes of the edge of the FITC–Dx70 dye column were recorded without disturbing the image alignment with the brightfield image.

The images were analyzed by drawing a line along the EC surface under brightfield (Fig. 3A) and then overlaying this line on the fluorescence image (Fig. 3B). The radial distribution of fluorescence

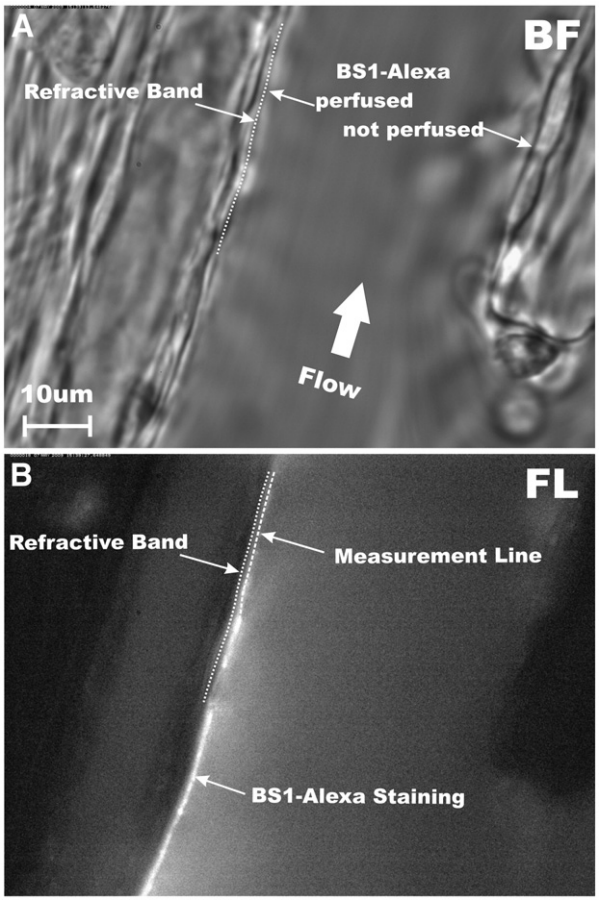

Fig. 2. Fluorescent labeling of the endothelial cell (EC) glycocalyx. (A) Brightfield image of a post-capillary venule (diameter = 40.7 μm). The plasma membrane of the EC was taken as the outermost edge of the dark refractive band between the EC and plasma layer. (B) Fluorescence image 10 min following proximal micropipette infusion of BS1-Alexa lectin. In this example fluorescence was confined to the left microvessel wall due to heterogeneity of network perfusion. A measurement line was drawn along the left EC wall and fluorescence intensity was averaged over an area within 0.5 μm on either side of the measurement line.

intensity was then obtained along a radial measurement line with its center on, and normal to, the EC boundary line, as shown in Fig. 3B. This radial measurement line was moved along the EC boundary line to acquire a radial distribution at each pixel of the boundary line and calculate an average radial intensity profile for up to 1600 locations along the boundary (symbols in Fig. 3C). The radial distribution of intensity was then fit with a 5-parameter sigmoidal curve, $I = I_0 + a\left(1 + e^{\frac{r-r_0}{b}}\right)^{-c}$ (solid line in Fig. 3C). The inflection point of this curve (IP) was calculated from the curve fit parameters as $IP = r_0 + b \cdot \ln(c)$and taken as the location of the edge of the glycocalyx. The distance between the EC wall and IP was taken as the thickness of the glycocalyx layer. All image processing and measurements were done using ImageJ (NIH, Bethesda, MD).

Diffusion coefficient measurement

The diffusion of a small solute (FITC) through the glycocalyx was characterized by measurement of its concentration (fluorescence intensity) in the radial direction as a function of time near the EC surface of post-capillary venules. Using measured values of fluorescence intensity at known distances from the EC as they varied with time, an effective diffusion coefficient (D) was computed from the equation governing one-dimensional diffusion in a homogenous medium. Free FITC solution was given as a systemic bolus (0.16 mL at 1.875 mL/min) using a syringe pump (PhD2000 Programmable,

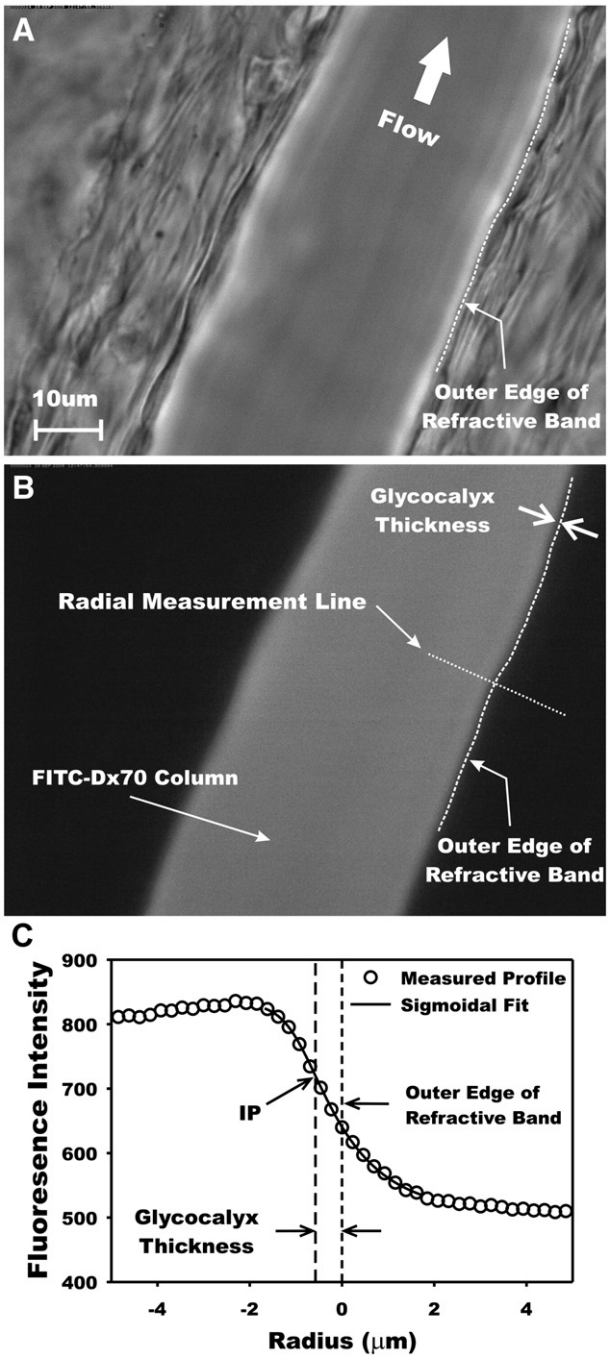

Fig. 3. Measurement of glycocalyx thickness. (A) Brightfield image of a post-capillary venule (dia = 35 μm) after a 0.15 mL systemic FITC–Dx70 bolus injection. The outermost edge of the dark refractive band was taken as the surface of the EC. (B) Fluorescence micrograph with circulating FITC–Dx70. (C) Fluorescence intensity distribution (open symbols) along a radial measurement line was fit with a sigmoidal curve (solid line) to determine its inflection point, IP. The distance between the IP and the EC surface was taken as the thickness of the glycocalyx.

Harvard Apparatus, Holliston, MA) via the jugular vein catheter. The first 10 s of the fluorescent bolus passing through the venular section was recorded at 2 frames/s (500 ms exposure time per frame). Brightfield images were recorded following the bolus to locate the EC surface. The radial intensity profiles over 1 μm distance from the EC boundary was recorded with a spatial resolution of 17.3 pixel/μm to obtain the transient distribution of intensity, $I(r,t)$ along a 1 pixel wide line normal to the wall. The intensities recorded at the location of the edge of the glycocalyx (determined from previous Dx70 measurements) $I(\delta,t)$, were used as the boundary conditions for a computational model of quasi-1-D transient diffusion through a porous layer bounding the EC surface. The diffusion coefficient, D, of FITC molecules inside the glycocalyx was estimated by determining the value of D which yielded the best agreement of computed and measured distributions of $I(r,t)$. This process was repeated for three locations within the field of view and averaged to obtain a value representative of the microvessel.

The transient diffusion of a solute of concentration $c(r,t)$ through a porous layer of thickness δ was obtained from the one-dimensional diffusion equation, non-dimensionalized in time, radial distance and concentration to yield,

$$\frac{\partial\theta}{\partial\tau} = \frac{\partial^2\theta}{\partial\eta^2} \tag{1}$$

where the dimensionless parameters are $\theta = \frac{c}{c_m}$, $\eta = \frac{r}{\delta}$, $\tau = \frac{t\cdot D}{\delta^2}$, D is the diffusion coefficient, and c_m is the maximum concentration of solute at the edge of the glycocalyx, $r=\delta$, and $r=0$ at the EC surface. The initial concentration within the layer was taken as $c(r,0)=0$, and the concentration at the outer edge, $c_\delta = c(\delta,t)$, was taken from measurements. The concentration of solute, $c(r,t)$, was assumed to be linearly proportional to fluorophore intensity, $I(r,t)$, for which the background intensity at each pixel was subtracted off using values taken under fluorescence illumination immediately prior to entry of FITC into the video field.

The differential equation and boundary conditions were rewritten into finite difference equations with 2nd order accuracy in space and time. Eq. (1) was solved using a fully implicit computation scheme in MatLab (The MathWorks Inc., Natick, MA), for specified values of $c_\delta(t)$ and D. The surface depicting a solution of $c(r,t)$ was compared with the experimental measurements of $I(r,t)$ by computing the root mean square (RMS) error $\varepsilon = \sqrt{\frac{1}{N}\sum\left(1-\frac{c(r,t)}{I(r,t)}\right)^2}$, where N is the total number of measured data points. An iterative method was used to determine the diffusion coefficient that yielded a minimum in the RMS error which was selected as the solution. The precision of this technique enabled resolution of D to within a numerical error of 0.5%.

Statistical methods

Statistical analyses of the data were performed using SigmaStat 3.0, SPSS Inc. Multiple comparison of different treatments were performed using the Student–Newman–Keuls test for one-way ANOVA. Statistical significance was asserted when the probability of the null hypothesis being true was $p<0.05$. Statistics of vessel diameters for all three protocols, glycocalyx thickness and goodness of fit (RMS error) for diffusion coefficient measurements are listed in Table 1.

Results

Enzymatic removal of BS1 labeled GAGs

Presented in Fig. 4 are ratios of the intensity of the BS1-Alexa stain to its respective control for no stimulus and following enzyme perfusion. The control measurements ($I_{Control}$) were taken at a time of 30–40 min following introduction of the BS1 which corresponds to the cumulative elapsed time between labeling, intubation of the venule and 10 min of enzyme perfusion. The fluorescence intensity of BS1-Alexa decreased significantly after perfusion with each enzyme, $p<0.05$. Under conditions of no stimulus, natural shedding of the glycocalyx components caused the fluorescence to decrease to 89.5 ± 8.0SD% of control in a 40 min period. By comparison, during the same length of time, enzyme perfusion induced significantly greater reductions to: 37.1 ± 7.7SD% with heparinase, 43.0 ± 6.9SD% with chondroitinase and 65.6 ± 7.4SD% with hyaluronidase. Superfusion

Table 1
Statistics of vessel diameters and curve fits determining the boundary of the glycocalyx and the diffusion coefficient of FITC.

	Treatment	Control	Heparinase	Chondroitinase	Hyaluronidase	Enzyme mix	fMLP
(A) BS1 cleavage assay	*n*	12	8	8	12		11
	Diameter (μm)	42.6 ± 6.19	45.4 ± 8.1	47.2 ± 8.3	44.6 ± 7.1		42.1 ± 11.4
(B) Sigmoidal fits of FITC–Dx70 radial intensity *	*n*	77	14	17	16	17	13
	Diameter (μm)	38.3 ± 7.58	37.8 ± 10.3	40.0 ± 8.5	39.9 ± 6.2	36.9 ± 5.7	36.2 ± 5.2
(C) Intensity–distance–time fits for diffusion coefficient calculation	*n*	10	7	7	8		9
	Diameter (μm)	25.5 ± 5.9	27.7 ± 8.1	38.3 ± 10.8	35.7 ± 13.3		27.4 ± 7.4
	RMS error (%) D_{Dx70}	35.0 ± 0.9	33.8 ± 0.2%	33.9 ± 0.2	34.5 ± 0.6		34.2 ± 0.4
	RMS error (%) D_{173}	33.7 ± 0.2%	33.6 ± 0.1%	33.5 ± 0.1%	33.8 ± 0.2%		33.7 ± 0.2%

Data are mean ± SD.
In each case, all treatments were not statistically significant from control for diameter and goodness of fit.
* For all sigmoidal fits, $R^2 = 0.9998 \pm 0.0001$ SD.

with 10^{-7} M fMLP for 10 min resulted in a reduction in intensity to 64.5 ± 7.6SD%. This decrease was consistent with previous studies using BS1-FITC and superfusion with 10^{-7} M fMLP for 10 min (Mulivor and Lipowsky, 2004). Treating the glycocalyx with heparinase or chondroitinase leads to a significantly greater reduction in BS1 label compared with fMLP, but hyaluronidase did not.

Thickness of the glycocalyx layer

The apparent thickness of the glycocalyx estimated by Dx70 exclusion is shown in Fig. 5A for control conditions (no treatment), enzymatic removal of HS, CS and HA and superfusion with fMLP. Under control condition, the Dx70 exclusion thickness averaged 463.1 ± 146.1 SD nm, which was consistent with prior measurements using Dx70 (Vink and Duling, 2000). Enzymatic GAG shedding by heparinase, chondrotinase and hyaluronidase decreased the barrier thickness to 234.0 ± 106.0 SD nm, 285.6 ± 145.2 SD nm and 303.3 ± 165.8 SD nm, respectively. The greater decrease in thickness with heparinase, compared to chondroitinase and hyaluronidase, was not significantly different from the thickness corresponding to these two enzymes. When all three GAGs were removed by a mixture of the three enzymes (same concentration as used individually) the barrier thickness decreased to 51.8 ± 41.3 SD nm.

The fractional decreases in thickness ($\delta_{Treated}/\delta_{Control}$) are illustrated in Fig. 5B. Individually, the reductions in thickness for each enzyme were not significantly different from the 28% reduction incurred by superfusion with fMLP. The mixture of enzymes removed nearly 90% of the barrier thickness, i.e. $\delta_{Treated}/\delta_{Control} = 0.103 \pm 0.07$ SD.

Diffusion coefficient of FITC in the glycocalyx

Typical results for comparison of the computed and measured transient diffusion of FITC into the glycocalyx are shown in Fig. 6. The shaded region shows the radial concentration profile with time,

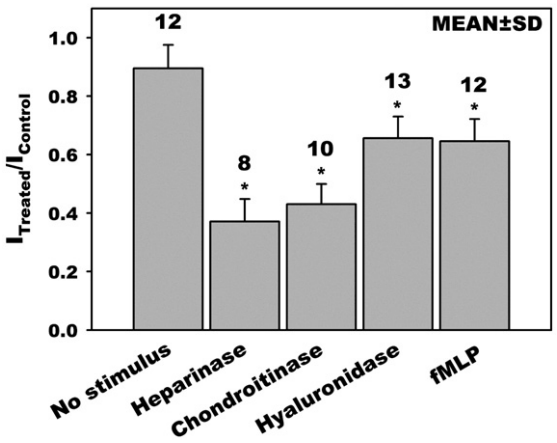

Fig. 4. Fluorescence intensity of BS1-Alexa along the endothelial surface of post-capillary venules 30–40 min following proximal infusion of the lectin with a micropipette. Control measurements were taken 10 min prior to each treatment. Intensities were normalized with respect to control, $I_{Treated}/I_{Control}$. Intensity of the fluorescent stain fell 15% with no stimulus, due to natural shedding of glycans. Following 10 min of enzymatic degradation with heparinase, chondroitinase and hyaluronidase, and superfusion of the mesentery with fMLP, glycan labeling was reduced significantly compared to natural shedding (no stimulus), $^*p<0.05$.

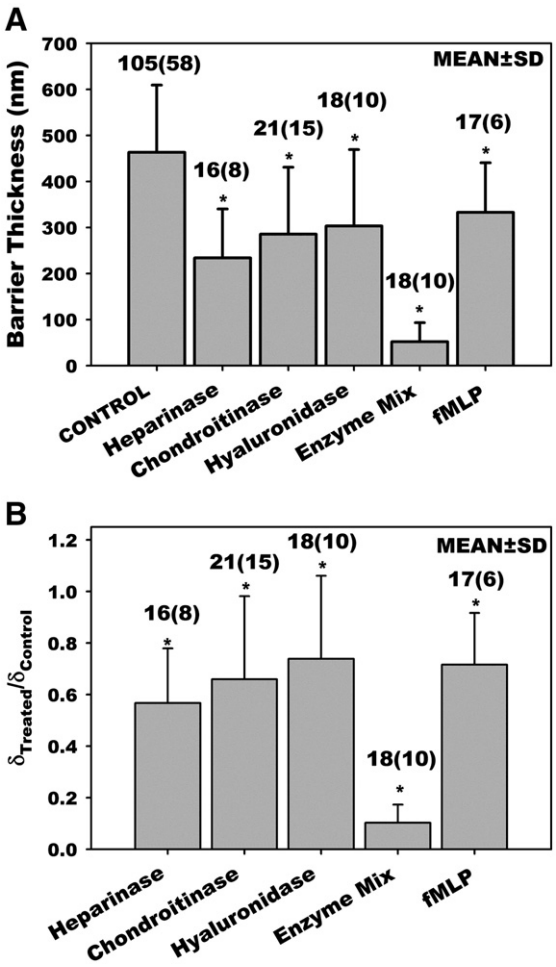

Fig. 5. Estimation of the thickness of the glycocalyx from the thickness of the barrier to infiltration of FITC–Dx70. (A) Thickness measurements taken as the distance between the inflection point in the radial intensity profile at the wall and the EC surface, for control (no perfusion) and micropipette perfusion with the indicated enzymes, and superfusion with fMLP. (B) Ratio of the post to pre-treatment thickness, $\delta_{Treated}/\delta_{Control}$. The number of observations is given along with the number of post-capillary venules (in parenthesis). All treatments caused a significant decrease ($^*p<0.05$) relative to control measurements.

computed using the fluorescence intensity-time curve measured at the edge of the glycocalyx ($r=462$ nm, control in Fig. 5A). The EC luminal surface is at $R=0$. Measured fluorescence intensities (symbols) agreed with the computational model to within an RMS error of 34.6%. The greatest errors in the fit appear to occur near the wall as the concentration of the FITC accumulates at maximal time, and scattered light or possible dye leakage through the wall interferes with the measurements. In this example, the best fit solution was obtained for a diffusion coefficient of 2.61×10^{-9} cm^2/s.

To explore the heterogeneity of the glycocalyx structure, two different boundary conditions were employed for calculation of the diffusion coefficient for all treatments: (a) Using the intensity-time curve at $r=\delta$, where δ was determined by the Dx70 exclusion, and (b) using the intensity-time curve at 4 pixels from the EC surface ($r=173$ nm from the EC surface). This latter sublayer represented the minimum number of pixels (thickness) needed to compute the transient dye concentration profile. Results for computation of D based on the Dx70 exclusion thickness (D_{Dx70}) are shown in Fig. 7A for all treatments. Under control conditions ($\delta=462$ nm), D_{Dx70} for FITC equaled $2.30\pm0.44\times10^{-9}$ cm^2/s, which was three-orders less than its free diffusion coefficient of 2.7×10^{-6} cm^2/s. After application of chondroitinase and hyaluronidase, D_{Dx70} increased significantly to $3.27\pm0.89\times10^{-9}$ and $3.24\pm1.28\times10^{-9}$ cm^2/s, respectively, roughly a 1.4-fold increase. However, decreases were found following heparinase ($1.37\pm0.35\times10^{-9}$ cm^2/s) and fMLP ($1.90\pm0.38\times10^{-9}$ cm^2/s) treatments.

Diffusion coefficients for the sublayer at 173 nm from the EC surface (D_{173}) are shown in Fig. 7B. Under control conditions, D_{173} was on the order of 1×10^{-9} cm^2/s, which was roughly half of the D_{Dx70}, suggesting a more compact sublayer. In contrast, D_{173} for heparinase treatment was not significantly different from control ($p=0.860$), and was only 25% less than that for the Dx70 thickness. Treatment with chondroitinase and hyaluronidase resulted in an increase in D_{173} to on the order of 2×10^{-9} cm^2/s compared to control. Within the sublayer, the effect of fMLP was similar to that of heparinase. These relative changes are addressed in the Discussion. The statistics of vessels size and goodness of the fits are summarized in Table 1.

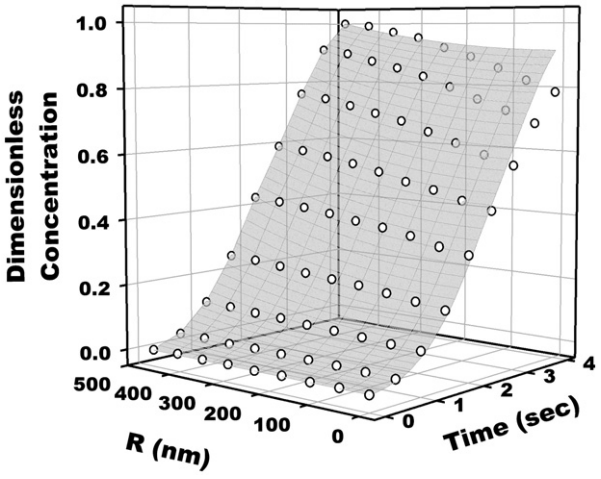

Fig. 6. Radial concentration at the wall of a post-capillary venule following systemic infusion (jugular vein, i.v.) of a small solute (FITC). Measured fluorescence intensity profiles (○) were obtained with time, normal to venular wall. The shaded surface represents the solution to the 1-D diffusion model, computed using the measured intensity-time curve at a distance δ from the wall, determined by the exclusion of FITC–Dx70 (Fig. 5). In this illustrative case, the experimental data and the computational prediction agreed within an RMS error of 34.6%, and correspond to a diffusion coefficient for FITC of 2.61×10^{-9} cm^2/s.

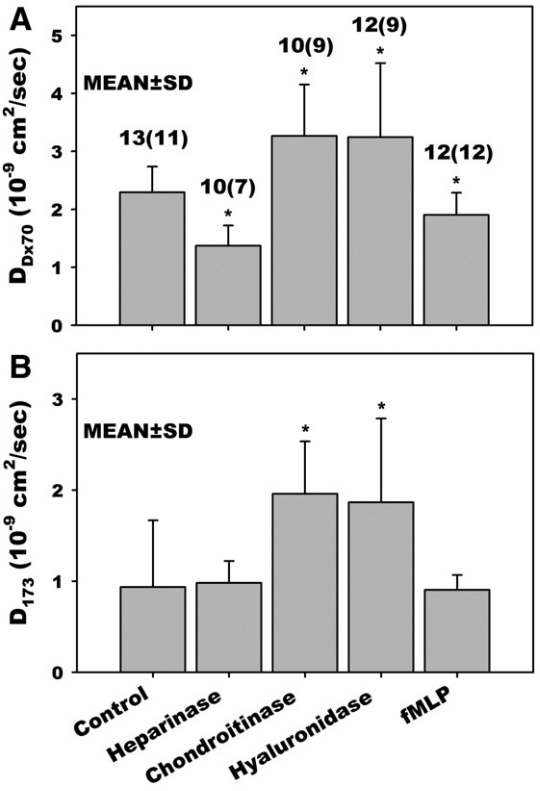

Fig. 7. Calculated diffusion coefficient, D, of FITC in the glycocalyx obtained from a model of unsteady one-dimensional diffusion normal to the EC surface. (A) Diffusion coefficient (D_{Dx70}) from solution of the diffusion equation based upon time variation of FITC concentration at a distance from the EC surface equal to the exclusion thickness of Dx70. (B) Diffusion coefficient (D_{173}) assessed for a sublayer 173 nm above the EC surface. Neither heparinase nor fMLP significantly affected D_{173}. The number of observations is given along with the number of post-capillary venules in parentheses. *Significantly different from control, $p<0.05$.

Discussion

The present studies have aimed to delineate the relative contributions of the three principal GAGs which serve as a barrier to transvascular exchange of macromolecules and leukocyte–endothelium adhesion. The lability of the glycocalyx has been shown previously in models of inflammation by topical application of either the cytokine TNF-α (Henry and Duling, 2000) or the chemoattractant fMLP (Mulivor and Lipowsky, 2004). In the latter case, rapid shedding of glycans was indicated by a reduction in the bound fluorescent lectin BS1. Given the permissive nature of lectin binding (Schnitzer et al., 1990) and the increase of circulating HA found in response to stimuli such as shear and oxidative stress (Gouverneur et al., 2006) and hyperglycemia (Nieuwuwdorp et al., 2006), the effectiveness of enzymatically removing the BS1 stained glycocalyx was compared with the acute fMLP response (Fig. 4). The results of these experiments suggest that heparinase, chondroitinase and hyaluronidase are equal to or greater in cleaving their respective targets compared with the physiologically induced shedding by fMLP. Although the binding and staining of lectin to each of the GAG species may not be in proportion to GAG concentration, the slightly greater decrease in HS-bound lectin compared to that bound to CS is consistent with prior studies of the greater amounts of HS compared to CS. It has been shown that in the case of HS and CS bound to syndecans, there exists one or two CS chains for every four HS chain (Rapraeger and Bernfield, 1985).

Building upon techniques established by Vink and Duling (1996, 2000), a measure of the thickness of the glycocalyx was derived from the depth of infiltration of Dx70 which was consistent with their

measurements for the undisturbed surface layer thickness, δ. Prior reports of the effect of hyaluronidase on δ are similar in many respects, albeit derived using other methods (systemic infusion vs. direct perfusion of individual microvessels), different species (hamster or mouse vs. rat), and/or different classes of microvessels (arterioles, capillaries or venules). Henry and Duling showed that systemic infusion of hyaluronidase for 1 h resulted in a 35% reduction in δ in small post-capillary venules (10–15 μm) (Henry and Duling, 1999) which was equivalent to the decrease found herein by 10 min of direct perfusion using micropipettes in larger venules (14–60 μm). A similar loss of δ in response to infusion of hyaluronidase was inferred by the indirect technique of particle image velocimetry by extrapolation of venular velocity profiles in cremaster muscle (Potter and Damiano, 2008). The uniqueness of the present study is its attempt to make a systematic comparison of the individual contribution of all three GAGs to the barrier thickness in post-capillary venules where physiological shedding of glycans have been shown to govern the adhesion of leukocytes in models of inflammation and ischemia (Mulivor and Lipowsky, 2004).

Enzyme specificity

Interpretation of the effect of each enzyme treatment needs to be made in light of their specificity for each GAG. It has been shown that heparinase III only cleaves HS and does not react with CS or HA (Lohse and Linhardt, 1992). However, hyaluronidase can degrade CS and chondroitinase can degrade HA. As a result, the chondroitinase or hyaluronidase treatments may not lead to exclusive degradation of CS or HA. To address the possible cross-reactivity, all three enzymes were mixed and applied to the venular glycocalyx to degrade all three GAGs, as shown in Fig. 5B. The thickness of the glycocalyx was reduced dramatically to 10.3% of the control for an 89.7% loss. By comparison, the percentage loss in thickness for individual enzymes was 43.3%, 34.1% and 26.1% for heparinase, chondroitinase and hyaluronidase, respectively. A simple model can be applied to attribute the loss in layer thickness to the fractional reduction of each individual GAG by assuming that the loss of each specific GAG is proportional to the decrease in glycocalyx thickness caused by each specific enzyme. A set of simultaneous algebraic equations may be written if one assumes that the specificity of each enzyme is such that: (1) All enzymatic degradations are maximal, (2) chondrotinase does not degrade HA significantly due to the low rate of enzymatic activity against HA (Hamai et al., 1997), and (3) hyaluronidase can cross-react with CS (Volpi et al., 1995). Based upon the data in Fig. 5, the percentage loss (PL) of the barrier thickness corresponding to each enzyme may then be expressed by the following equations:

$$PL_{HS} = 1-\delta_{Heparinase} / \delta_{Control} = 43.3\% \quad (2)$$

$$PL_{CS} = 1-\delta_{Chondroitinase} / \delta_{Control} = 34.1\% \quad (3)$$

$$PL_{HS} + PL_{CS} = 1-\delta_{Hyaluronidase} / \delta_{Control} = 26.1\% \quad (4)$$

$$PL_{HS} + PL_{CS} + PL_{HA} = 1-\delta_{EnzymeMix} / \delta_{Control} = 89.7\% \quad (5)$$

where $PL_{CS'}$ refers to the percentage of the thickness reduction due to shedding of CS by hyaluronidase and the percentages on the right hand side are from Fig. 5B. Solution of these equations indicates that HS, CS and HA contributed 43.3%, 34.1% and 12.3% respectively to the barrier thickness, and collectively, the three GAGs account for 90% of the barrier thickness. Hyaluronidase also induced a major 13.8% ($PL_{CS'}$) drop in barrier thickness through cross-reacting with CS.

Thus, this simplified model suggests that HS provides the greatest contribution to the barrier thickness of the glycocalyx, followed by CS and HA. However, caution should be taken to interpret the reduction of 'barrier thickness' as reduction of 'glycocalyx thickness.' It has been shown that the magnitude of post-hyaluronidase reduction measured with Dx70 is similar to that with Dextran 145 kDa, but completely vanished when using larger molecular weight dextrans of 580 kDa or 2000 kDa (Henry and Duling, 1999), suggesting that infiltration of Dx70 may follow an increase of porosity, instead of a decrease in layer thickness.

Structural implications

The present results suggest a non-uniformity of GAG distribution through the depth of the glycocalyx. In control experiments, the significantly lower diffusion coefficient of FITC in the 173 nm thick sublayer compared to the value at the Dx70 exclusion thickness (463 nm) (Fig. 7) may reflect a non-uniform density of the glycocalyx. The difference suggests a denser sublayer that hinders FITC diffusion. The effective diffusion coefficient of small solutes in a porous media is proportional to the free media diffusion coefficient, porosity and constrictivity, and inversely proportional to the tortuosity of pathways. In a fibrous matrix such as the glycocalyx, the void volume is likely high enough to render the tortuosity as a trivial factor. The constrictivity is dependent upon size of the particle relative to the pore size. For FITC, with a Stokes–Einstein diameter of 1.68 nm, variations in pore size from 4 to 10 nm (Squire et al., 2001) may introduce significant heterogeneities in diffusion throughout the glycocalyx layer. The lower diffusion coefficient found in the sublayer is consistent with the their findings of a more compact layer near the EC surface, as indicated by greater staining of the glycocalyx 50–100 nm above the EC. This denser sublayer may result from continued biosynthesis of HA chains near the EC membrane and loss of distal GAGs by shear stress effects of blood flow on the outer boundary of the glycocalyx.

The variation of diffusion coefficient with specific enzyme treatment is also suggestive of the heterogeneity of GAG distribution. In Fig. 7, shedding of HS by heparinase failed to induce any change in the diffusion coefficient of the sublayer from the control. This suggests that HS predominantly resides in the top portion of the glycocalyx layer. In contrast, shedding of CS and HA both significantly increased the diffusion coefficient two-fold from control within the 173 nm sublayer, suggesting greater amounts of CS and HA. The overall distributions of CS and HA are also likely to be biased toward the EC surface, because after shedding by chondroitinase or hyaluronidase, D_{173} increased two-fold, but only by a factor of 1.4 for D_{Dx70}. This finding is consistent with previous studies on syndecan-1 proteoglycan (a major glycocalyx associated GAG carrier) that the HS attachment sites are closer to the N-terminal where the CS attachment sites are in the proximity of the transmembrane domain on the core protein (Kokenyesi and Bernfield, 1994). The observation that both D_{Dx70} and D_{173} increased dramatically from control after CS or HA was cleaved, but not with removal of HS, suggests that CS and HA contribute a significantly greater amount to glycocalyx permeability (by affecting the porosity of the glycocalyx layer) compared to HS.

The anomalous decrease in diffusion coefficient at the Dx-70 exclusion thickness with heparinase and fMLP may arise from structural rearrangements following the treatment. It is plausible that the layer collapses due to the loss of HS and associated macromolecules. In a previous study, Squire et al. (2001) observed reductions in the perpendicular spacings of the glycocalyx fiber matrix from 22.6 nm under control to 15.5 nm under inflammatory conditions. It would thus appear that HS could provide the structural support of the upper layer of the glycocalyx.

fMLP-induced shedding

Previous studies have shown that the glycocalyx is rapidly shed after 10 min application of fMLP (Mulivor and Lipowsky, 2004). In the present study, after 10 min fMLP superfusion, the glycocalyx thickness

was reduced from 463 nm to 332 nm, and the FITC diffusion coefficient (D_{Dx70}) across the glycocalyx layer decreased from 2.3 to 1.9×10^{-9} cm^2/s. Thus it appears that fMLP decreased both barrier thickness and porosity. The combination of these two counteracting effects may result in no significant net change in the solute permeability across the layer. Previous studies have shown that fMLP alone was unable to change endothelial permeability, despite the fact that glycocalyx was lost (Zhu et al., 2005). The pattern of change in diffusion coefficient by fMLP is similar to heparinase, in which both treatments reduced D_{Dx70} but not D_{173}. However, further studies are needed to determine if the dominant GAG loss with fMLP is heparan sulfate in contrast to chondroitin sulfate or hyaluronan.

In conclusion, this study has measured relative GAG shedding using the lectin BS-1, Dx70 exclusion thickness and the diffusion coefficient of FITC at a 173 nm basal sublayer and the Dx70 exclusion thickness under control, fMLP-induced inflammation as well as post-enzymatic degradation of GAGs by heparinase III, chondroinase ABC and hyaluronidase. It is suggested that HS may be the primary GAG being shed during fMLP-induced inflammatory response. Analysis of the results suggests three updates to prevailing structural models of the glycocalyx: (1) GAGs are not evenly distributed throughout the glycocalyx, HS is distributed predominately on the luminal side of the glycocalyx layer, and the EC-adjacent sublayer is dominated by CS and HA; (2) A denser EC-adjacent sublayer exists that is likely on the order of 200 nm and (3) HS plays a dominant role in the structural integrity of the glycocalyx and chondroitin sulfate and hyaluronan contribute significantly to its permeability.

Acknowledgments

The authors appreciate the technical assistance of Ms. Anne Lescanic. This work supported by NIH Research Grant HL-39286-20.

References

Adamson, R.H., 1990. Permeability of frog mesenteric capillaries after partial pronase digestion of the endothelial glycocalyx. J. Physiol. 428, 1–13.
Adamson, R.H., Clough, G., 1992. Plasma proteins modify the endothelial cell glycocalyx of frog mesenteric microvessels. J. Physiol. 445, 473–486.
Aruffo, A., Stamenkovic, I., Melnick, M., Underhill, C.B., Seed, B., 1990. CD44 is the principal cell surface receptor for hyaluronate. Cell 61, 1303–1313.
Bruegger, D., Jacob, M., Rehm, M., Loetsch, M., Welsch, U., Conzen, P., Becker, B.F., 2005. Atrial natriuretic peptide induces shedding of endothelial glycocalyx in coronary vascular bed of guinea pig hearts. Am. J. Physiol. Heart Circ. Physiol. 289, H1993–H1999.
Chappell, D., Hofmann-Kiefer, K., Jacob, M., Rehm, M., Briegel, J., Welsch, U., Conzen, P., Becker, B.F., 2009. TNF-alpha induced shedding of the endothelial glycocalyx is prevented by hydrocortisone and antithrombin. Basic Res. Cardiol. 104, 78–89.
Constantinescu, A.A., Vink, H., Spaan, J.A., 2001. Elevated capillary tube hematocrit reflects degradation of endothelial cell glycocalyx by oxidized LDL. Am. J. Physiol. Heart Circ. Physiol. 280, H1051–H1057.
Florian, J.A., Kosky, J.R., Ainslie, K., Pang, Z., Dull, R.O., Tarbell, J.M., 2003. Heparan sulfate proteoglycan is a mechanosensor on endothelial cells. Circ. Res. 93, e136–e142.
Gouverneur, M., Spaan, J.A., Pannekoek, H., Fontijn, R.D., Vink, H., 2006. Fluid shear stress stimulates incorporation of hyaluronan into endothelial cell glycocalyx. Am. J. Physiol. Heart Circ. Physiol. 290, H458-2.
Haldenby, K.A., Chappell, D.C., Winlove, C.P., Parker, K.H., Firth, J.A., 1994. Focal and regional variations in the composition of the glycocalyx of large vessel endothelium. J. Vasc. Res. 31, 2–9.
Hamai, A., Hashimoto, N., Mochizuki, H., Kato, F., Makiguchi, Y., Horie, K., Suzuki, S., 1997. Two distinct chondroitin sulfate ABC lyases. An endoeliminase yielding tetrasaccharides and an exoeliminase preferentially acting on oligosaccharides. J. Biol. Chem. 272, 9123–9130.
Henry, C.B., Duling, B.R., 1999. Permeation of the luminal capillary glycocalyx is determined by hyaluronan. Am. J. Physiol. 277, H508–H514.
Henry, C.B., Duling, B.R., 2000. TNF-alpha increases entry of macromolecules into luminal endothelial cell glycocalyx. Am. J. Physiol. Heart Circ. Physiol. 279, H2815–H2823.
Hofmann-Kiefer, K.F., Kemming, G.I., Chappell, D., Flondor, M., Kisch-Wedel, H., Hauser, A., Pallivathukal, S., Conzen, P., Rehm, M., 2009. Serum heparan sulfate levels are elevated in endotoxemia. Eur. J. Med. Res. 14, 526–531.
Huxley, V.H., Curry, F.E., 1991. Differential actions of albumin and plasma on capillary solute permeability. Am. J. Physiol. 260, H1645–H1654.
Huxley, V.H., Williams, D.A., 2000. Role of a glycocalyx on coronary arteriole permeability to proteins: evidence from enzyme treatments. Am. J. Physiol. Heart Circ. Physiol. 278, H1177–H1185.
Kokenyesi, R., Bernfield, M., 1994. Core protein structure and sequence determine the site and presence of heparan sulfate and chondroitin sulfate on syndecan-1. J. Biol. Chem. 269, 12304–12309.
Laurent, T.C., Fraser, J.R., 1992. Hyaluronan. FASEB J. 6, 2397–2404.
Lohse, D.L., Linhardt, R.J., 1992. Purification and characterization of heparin lyases from Flavobacterium heparinum. J. Biol. Chem. 267, 24347–24355.
Mulivor, A.W., Lipowsky, H.H., 2002. Role of glycocalyx in leukocyte-endothelial cell adhesion. Am. J. Physiol. Heart Circ. Physiol. 283, H1282–H1291.
Mulivor, A.W., Lipowsky, H.H., 2004. Inflammation- and ischemia-induced shedding of venular glycocalyx. Am. J. Physiol. Heart Circ. Physiol. 286, H1672–H1680.
Mulivor, A.W., Lipowsky, H.H., 2009. Inhibition of glycan shedding and leukocyte-endothelial adhesion in postcapillary venules by suppression of matrix metalloprotease activity with doxycycline. Microcirculation 16, 657–666.
Nieuwdorp, M., van Haeften, T.W., Gouverneur, M.C., Mooij, H.L., van Lieshout, M.H., Levi, M., Meijers, J.C., Holleman, F., Hoekstra, J.B., Vink, H., Kastelein, J.J., Stroes, E.S., 2006. Loss of endothelial glycocalyx during acute hyperglycemia coincides with endothelial dysfunction and coagulation activation in vivo. Diabetes 55, 480–486.
Potter, D.R., Damiano, E.R., 2008. The hydrodynamically relevant endothelial cell glycocalyx observed in vivo is absent in vitro. Circ. Res. 102, 770–776.
Prehm, P., 1989. Identification and regulation of the eukaryotic hyaluronate synthase. Ciba Found. Symp. 143, 21–30.
Rapraeger, A., 1989. Transforming growth factor (type beta) promotes the addition of chondroitin sulfate chains to the cell surface proteoglycan (syndecan) of mouse mammary epithelia. J. Cell Biol. 109, 2509–2518.
Rapraeger, A., Bernfield, M., 1985. Cell surface proteoglycan of mammary epithelial cells. Protease releases a heparan sulfate-rich ectodomain from a putative membrane-anchored domain. J. Biol. Chem. 260, 4103–4109.
Rehm, M., Bruegger, D., Christ, F., Conzen, P., Thiel, M., Jacob, M., Chappell, D., Stoeckelhuber, M., Welsch, U., Reichart, B., Peter, K., Becker, B.F., 2007. Shedding of the endothelial glycocalyx in patients undergoing major vascular surgery with global and regional ischemia. Circulation 116, 1896–1906.
Reitsma, S., Slaaf, D.W., Vink, H., van Zandvoort, M.A., oude Egbrink, M.G., 2007. The endothelial glycocalyx: composition, functions, and visualization. Pflugers Arch. 454, 345–359.
Schnitzer, J.E., Shen, C.P., Palade, G.E., 1990. Lectin analysis of common glycoproteins detected on the surface of continuous microvascular endothelium in situ and in culture: identification of sialoglycoproteins. Eur. J. Cell Biol. 52, 241–251.
Scott, J.E., Heatley, F., 1999. Hyaluronan forms specific stable tertiary structures in aqueous solution: a 13C NMR study. Proc. Natl. Acad. Sci. USA 96, 4850–4855.
Squire, J.M., Chew, M., Nneji, G., Neal, C., Barry, J., Michel, C., 2001. Quasi-periodic substructure in the microvessel endothelial glycocalyx: a possible explanation for molecular filtering? J. Struct. Biol. 136, 239–255.
Stace, T.M., Damiano, E.R., 2001. An electrochemical model of the transport of charged molecules through the capillary glycocalyx. Biophys. J. 80, 1670–1690.
Sugihara-Seki, M., Akinaga, T., Itano, T., 2008. Flow across microvessel walls through the endothelial surface glycocalyx and the interendothelial cleft. J. Fluid Mech. 601, 229–252.
Svennevig, K., Hoel, T., Thiara, A., Kolset, S., Castelheim, A., Mollnes, T., Brosstad, F., Fosse, E., Svennevig, J., 2008. Syndecan-1 plasma levels during coronary artery bypass surgery with and without cardiopulmonary bypass. Perfusion 23, 165–171.
Toole, B.P., 1990. Hyaluronan and its binding proteins, the hyaladherins. Curr. Opin. Cell Biol. 2, 839–844.
Van den Berg, B.M., Vink, H., Spaan, J.A., 2003. The endothelial glycocalyx protects against myocardial edema. Circ. Res. 92, 592–594.
van Haaren, P.M., VanBavel, E., Vink, H., Spaan, J.A., 2003. Localization of the permeability barrier to solutes in isolated arteries by confocal microscopy. Am. J. Physiol. Heart Circ. Physiol. 285, H2848–H2856.
Vink, H., Duling, B.R., 1996. Identification of distinct luminal domains for macromolecules, erythrocytes, and leukocytes within mammalian capillaries. Circ. Res. 79, 581–589.
Vink, H., Duling, B.R., 2000. Capillary endothelial surface layer selectively reduces plasma solute distribution volume. Am. J. Physiol. Heart Circ. Physiol. 278, H285–H289.
Vogl-Willis, C.A., Edwards, I.J., 2004. High-glucose-induced structural changes in the heparan sulfate proteoglycan, perlecan, of cultured human aortic endothelial cells. Biochim. Biophys. Acta 1672, 36–45.
Volpi, N., Sandri, I., Venturelli, T., 1995. Activity of chondroitin ABC lyase and hyaluronidase on free-radical degraded chondroitin sulfate. Carbohydr. Res. 279, 193–200.
Weinbaum, S., Zhang, X., Han, Y., Vink, H., Cowin, S.C., 2003. Mechanotransduction and flow across the endothelial glycocalyx. Proc. Natl Acad. Sci. USA 100, 7988–7995.
Zhu, L., Castranova, V., He, P., 2005. fMLP-stimulated neutrophils increase endothelial [Ca2+]i and microvessel permeability in the absence of adhesion: role of reactive oxygen species. Am. J. Physiol. Heart Circ. Physiol. 288, H1331–H1338.
Zuurbier, C.J., Demirci, C., Koeman, A., Vink, H., Ince, C., 2005. Short-term hyperglycemia increases endothelial glycocalyx permeability and acutely decreases lineal density of capillaries with flowing red blood cells. J. Appl. Physiol. 99, 1471–1476.